Sixth International Conference on Estuaries and Coasts (ICEC-2018), August 20-23, 2018, Caen, France

Efficient modelling of complex coastal evolution at monthly to century time scales

Dano Roelvink[*1,2,3], Bas Huisman[2,3], Ahmed Elghandour[1]

[1]*IHE Institute for Water Education, Delft, the Netherlands*
[2]*Deltares, Delft, the Netherlands*
[3]*Delft University of Technology, Delft, the Netherlands*

Abstract: With large-scale human interventions and climate change unfolding as they are now, coastal changes at decadal timescales are not limited to incremental modifications of systems that are fixed in their general geometry, but often show radical changes in layout that may be catastrophic for populations living in previously stable areas. This poses severe challenges that are difficult to meet for existing models. We present a new free-form coastline model, ShorelineS, that is capable to describe drastic coastal transformations based on relatively simple principles borrowed from general coastline theory (Pelnard-Considere, 1956) and the Coastal Evolution Model (Ashton et al., 2001). As in (Hurst et al., 2015) it is vector-based, describing the coastline like a freely moving string of points, but on top of this it allows for an arbitrary number of coast sections, which can be open or closed and can interact with each other, and rocky parts or structures. This allows for a rich behaviour including shoreline undulations and formation of spits, migrating islands, merging of coastal shapes, salient and tombolos. In the paper we describe in some detail the (open-source) Matlab-based model, present some principle test cases and a field validation for the case of the Sand Engine (Stive et al., 2013). We then refer to recent developments that will be published elsewhere and sketch some approaches towards including other processes (beach-dune interactions, interactions with tidal basins, probabilistic coastline recession) in simulating coastal evolution on decadal scales, and in light of climate change and population pressure. The open-source Matlab code and documentation is freely available at www.shorelines.nl.

Keywords: Coastal evolution, coastline model, spit, barrier, salient, tombolo

1. Introduction

Sandy beaches are extremely valuable natural resources, providing the first line of defence against coastal storm impacts, as well as other ecosystem services (Barbier et al., 2011) such as ecological habitats and recreation areas. They often are an essential part of nations' heritage. However, many of the world's coastlines suffer erosion, due to interruption of sand flows from upstream (Syvitski et al., 2005) and alongshore, sand mining and sea-level rise effects, especially in the vicinity of tidal inlets (Ranasinghe et al., 2013). A lack of reliable, widely usable models makes it difficult to develop sound, science-based strategies for managing complex sandy coasts. While the physics of beaches have been studied extensively (Roelvink and Reniers, 2011) and useful model concepts exist, these are either too complex and time-expensive to use for engineering application at larger scales, too simple or too schematic.

The first practical concept for predicting coastline change due to interruption of wave-driven longshore transport was developed by Pelnard-Considère (Pelnard-Considere, 1956), who derived a diffusion-type equation based on the assumptions of a small angle of incidence and a constant cross-shore profile shape. The first very limiting assumption was relaxed by numerical, one-dimensional (1D) model approaches, which were developed since the 1980's, e.g. GENESIS (Hanson, 1989), UNIBEST (Tonnon et al., 2017), LITPACK (Kristensen et al., 2016). These models also applied increasingly powerful, and more advanced physics-based approaches to estimate the transport rate as a function of incident wave conditions, sediment parameters and profile shape. However, the main characteristic of the transport curve as a function of the wave angle remained a sine curve, with a maximum at roughly 45 degrees. For relative angles beyond this critical angle, longshore transport decreases for increasing angles and the morphological behaviour of the coastline becomes fundamentally unstable.

While the existing numerical models had no real solution for this, the Coastal Evolution Model (CEM) proposed by (Ashton et al., 2001) addressed this point using a grid-based, upwind approach, which they showed to be able to explain a variety of coastal forms found in nature.

The high angle wave instability mechanism (HAWI) has been studied extensively through linear and non-linear stability analysis, e.g. (Falques and Calvete, 2004), (Falqués

Commented [AE1]: defence (British)

[*] Corresponding author. Email: d.roelvink@un-ihe.org

et al., 2017); the latter included both this and the low angle instability mechanism (LAWI) proposed by (Idier et al., 2011). These analyses pointed out the importance of the refraction on the foreshore of shoreline undulations, which generally stabilize the coastline relative to the original HAWI mechanism proposed by (Ashton et al., 2001).

The 1D model approaches so far address a single, possibly curving, coastline or disparate sections of coastline. However, there are many cases where islands, shoals and spits shield other parts of the coast from waves; where spits weld onto the coast to form lagoons that in turn may break up into different parts; where islands migrate towards the coast and weld onto it. A step towards a more flexible 1D approach was taken by (Hurst et al., 2015); however, their model was limited to a single coastline section.

One way to compute these complex coastal evolutions is to apply process-based, two-dimensional (horizontal) models which can produce realistic, detailed simulations of complex coastal forms over several years, as for the recent case of the 'Sand Engine' in Holland(Luijendijk et al., 2017), but this comes at great computational expense and requires considerable expertise. An effort to increase the robustness and reduce the expense was made by (Kaergaard and Fredsoe, 2013b); however, the computational expense still precludes application on the scales that are a focus here.

Thus, rather stuck with one approach which does not capture the complexity of coastal evolution and another which is too expensive, a new approach is needed to robustly follow such coastal features through complete lifecycles at reasonable computational cost.

We present a radically new method to hindcast and forecast coastline evolution, applicable for domains from local to regional and even global.

2. Model description

Introduction

To overcome the severe limitations of existing coastline models we developed a radically new Shoreline Simulation model (**ShorelineS**), which is aimed at predicting coastline evolution over periods of years to centuries. Its description of coastlines is of strings of grid points (see Figure 1) that can move around, expand and shrink freely; the model can have multiple sections which may be closed (islands, lagoons). Sections can develop spits and other features; they may break up or merge as the simulation continues.

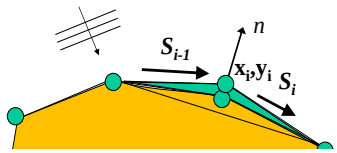

Figure 1 Coastline-following coordinates system

Basic equation

The basic equation for the updating of the coastline position is based on the conservation of sediment:

$$\frac{\partial n}{\partial t} = -\frac{1}{D_c}\frac{\partial Q_s}{\partial s} - \frac{c}{\tan\beta} RSLR + \frac{1}{D_c}\sum q_i$$

Here, n is the cross-shore coordinate, s the longshore coordinate, D_c the active profile height, Q_s the longshore transport (m^3/yr), c a coefficient, tan β the profile slope, *RSLR* the relative sea-level rise (m/yr) and q_i source/sink terms (m^3/m/yr) due to cross-shore transport, overwashing, nourishments, sand mining and exchanges with rivers and tidal inlets

Transport formulations

The coastline changes are driven by wave-driven longshore transport, which is computed using a choice of formulations, which can be calibrated to match the local transport rates. We have implemented the following formulations as shown in Table 1. The definitions of the angles are as in Figure 2.

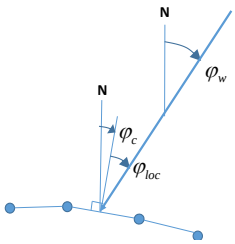

Figure 2 Definition of wave and coast angles

Table 1 Implemented longshore transport formulations

Author	Notation	Formula
USACE, 1984 (simplified)	CERC1	$Q_s = bH_{s0}^{5/2}\sin 2(\phi_{loc})$
Ashton & Murray, 2006	CERC2	$Q_s = K_2 H_{s0}^{\frac{12}{5}} T^{\frac{1}{5}} \cos^{\frac{6}{5}}(\phi_{loc})\sin(\phi_{loc})$
USACE, 1984	CERC3	$Q_s = b_1 H_{sb}^{5/2}\sin 2(\phi_{locb})$
Kamphuis, 1992	KAMP	$Q_s = 2.33 H_{sb}^2 T^{1.5} m_b^{0.75} D_{50}^{-0.25}\sin^{0.6}(2\phi_{locb})$

Where:

b : calibration coefficient CERC1

$b_1 = \frac{k\rho\sqrt{g/k}}{16(\rho_s-\rho)(1-p)}, k \sim 0.1-0.2$

$(\phi_{loc})_i^j = \arctan 2\left(\frac{\sin(\phi_c-\phi_w)}{\cos(\phi_c-\phi_w)}\right)_i^j$

$K_2 = (\frac{\sqrt{g\gamma}}{2\pi})^{\frac{1}{5}} K_1, K_1 \sim 0.4 m^{1/2}/s$

H_{s0} : offshore significant wave height

H_{sb} : significant breaking wave height

T : peak wave period

D_{50} : median grain diameter [m]

m_b : mean bed slope (beach slope in the breaking zone)

α_b : breaking wave angle

Here CERC1 and CERC2 are defined in terms of the offshore wave angle, and CERC3 and KAMP in terms of the breaking wave angle. However, in all cases the transport follows a shape rather similar to CERC1 when plotted against deep water wave angle, with a maximum occurring at an offshore angle of 40° -45°.

Numerical aspects

The ShorelineS model is implemented in Matlab. The coastline positions are given in column vectors *x_mc* and *y_mc*, where the different coast sections are separated by NaN's. The sea is defined to the left when following the coastline positions. Based on the initial coastline definition the grid points are generated with an initial user-specified grid size. After input definition and initialisations the time loop starts, during which for each time step a second loop is executed over all coast sections; in this loop, the following actions take place:

- Extract *x* and *y* of the local coast section;
- Check if grid sizes are bigger than half and smaller than twice the initial grid size; if not take out or insert a grid point.
- Find the offshore wave conditions, either from a time series or randomly selected from a given distribution;
- Compute the local wave angles;
- Compute longshore transport rates;
- For all transport points, check if they are in the shadow of other parts of the coast or of hard structures (see explanation below); in that case set transport to zero;
- For points where the local angle exceeds the angle of maximum transport, apply an upwind correction as in (Ashton et al., 2001)
- Set transport to zero where the coastline intersects a hard structure;
- Apply sources (nourishment) and sinks (e.g. dredging, loss to inlets, Bruun rule effect of RSLR);
- Apply boundary conditions: cyclic in case of islands, other options for unconnected sections;
- Apply coastline changes;
- Apply overwash mechanism as in (Lorenzo-Trueba and Ashton, 2014), as discussed below;
- Merge or split coastlines where necessary, taking into account also enclosed water bodies;

After the loop over all coast sections, we plot and store results, and continue the time loop. In the following we will detail a few important processes and algorithms.

Wave Shadowing

Some parts of the coastline might be sheltered by structures or other parts (sections) of the coast. Hard structures or rocky shores are represented by an arbitrary number of polylines, which shield waves and block longshore transport where they cross a coastline. The waves at any location can be shielded by other coast sections or hard structures, see Figure 3.

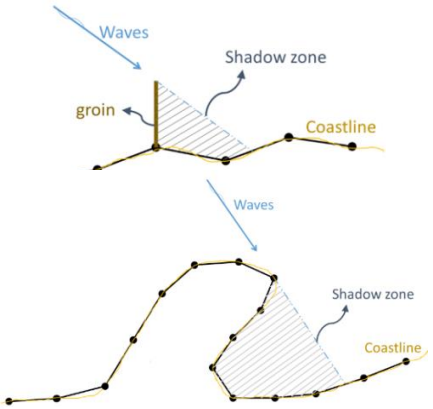

Figure 3 Areas affected by wave shadowing in case of hard structure (top panel) or other (part of) coast section (bottonm panel).

Coastline evolution

At each point the local direction of the coast is determined from the two adjacent points (as reference line), then the longshore transport is calculated for each segment; the difference leads the points to build out or to shrink.

The mass conservation equation is solved using a staggered forward time –central space explicit scheme (see Figure 1):

$$\Delta n_i^j = -\frac{1}{D_c}\frac{2(Q_{s.i}^j - Q_{s,i-1}^j)}{L_i}\Delta t$$

Here:

j = time step index

Δt = time step

i = point/node index

$$L_i = \sqrt{(x_{i+1} - x_{i-1})^2 + (y_{i+1} - y_{i-1})^2}$$

From the normal displacement it follows that the change in position of point i then becomes:

$$\Delta x_i^j = -\Delta n_i^j \left(y_{i+1} - y_{i-1} \right) / L_i$$

$$\Delta y_i^j = \Delta n_i^j \left(x_{i+1} - x_{i-1} \right) / L_i$$

$$x_i^{j+1} = x_i^j + \Delta x_i^j$$

$$y_i^{j+1} = y_i^j + \Delta y_i^j$$

The scheme can be shown to be conserving the land area.

High-angle instability

A special treatment takes care of so-called high-angle instability (Ashton et al., 2001), which allows spits to develop. In cases where the local angle exceeds the critical angle on one side and is less than the critical angle at the updrift side, the transport at the downdrift point is set to the maximum transport (or the angle set to the critical angle). Figure 4 illustrates the effect of this treatment, where a central scheme would lead to unstable behaviour, the local upwind treatment ensures a smooth development into a spit.

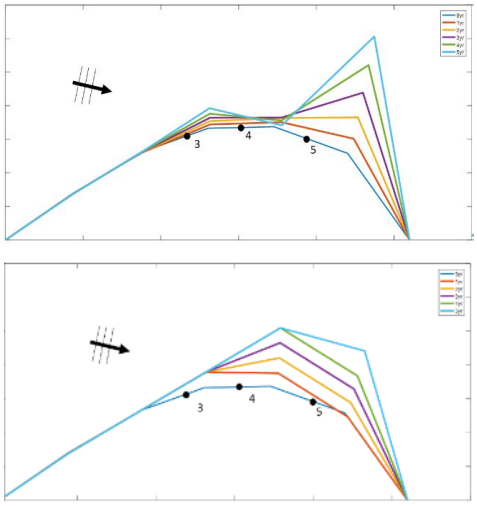

Figure 4 Example of high-angle instability with standard central scheme (top panel) and upwind scheme (bottom panel).

Barrier or spit overwash

For simulating barriers that already exist or in the form of developed spits due to high wave angle instability, it was necessary to represent the overwash process as it maintains the width of the barrier to a certain limit (Leatherman, 1979).

(Ashton & Murray, 2006a) introduced an analytical solution for maintaining a minimum barrier width by overwashing. By simultaneously retreating the seaward and landward side of a section narrower than the specified critical width, the retreated section creates a longshore transport gradient that tends to fill it up; thus the retreating helps maintain the width.

A similar concept was implemented in ShorelineS in a simple approach for treating the barrier width:

At each time step, the model checks the local barrier width at each point/node, measured in the incident wave direction. If the barrier is narrower than critical width the overwash occurs. The overwash process extends the point landward a distance equal to the difference between actual width and the critical width. Such distance cannot exceed 10% of the local spatial discretization distance of the grid per each time step to avoid discretization artefacts. Then the model looks for the closest node seaward to produce erosion by the same amount (Figure 5)

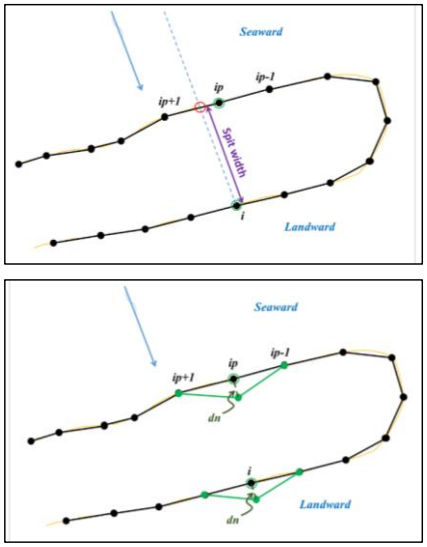

Figure 5 Overwash process in ShorelineS: check spit width (left panel), spit shifting landward (right panel).

Merging and splitting

One of the advantages of the ShorelineS model is that it can simulate multiple coastal sections at the same time, and those sections could affect each other by shielding the waves.

Small parts of the coast are allowed to split and migrate as the spits are growing and in some cases break up and migrate as a small island. An example of the splitting procedure is shown in Figure 7.

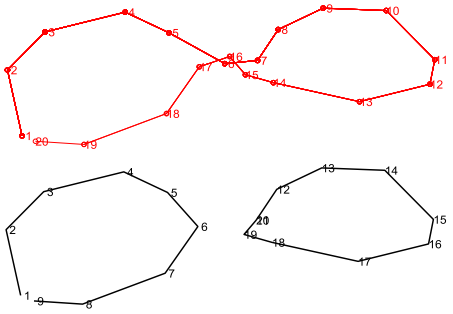

Figure 7 Illustration of splitting procedure; top panel, before splitting; bottom panel, after splitting.

If two sections intersect, they may merge into one section as the simulation continues, as is illustrated in Figure 8.

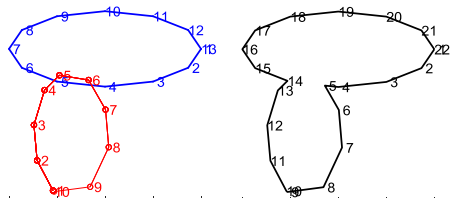

Figure 8 Illustration of two coast sections merging into one; left panel: two numbered sections before merge; right panel: after merging.

3. Principle tests

Island merging

This test has been designed to examine the model stability and behaviour under the merging and splitting of different coastal sections and to examine the upwind correction implementation.

The initial setup is a sandy island and a 10 km straight coast, with the mean wave direction from the north and randomly varying by +/- 15°, Hs = 1.4m, Tp = 6s. The test was performed with the four formulas implemented, the cartoon in Figure 9 showing the test using Kamphuis equation. We see from top to bottom: the initial condition; formation of island spits; welding to the coast creating a lagoon; breaking through of the lagoon; re-closure and finally longshore diffusion of the sand

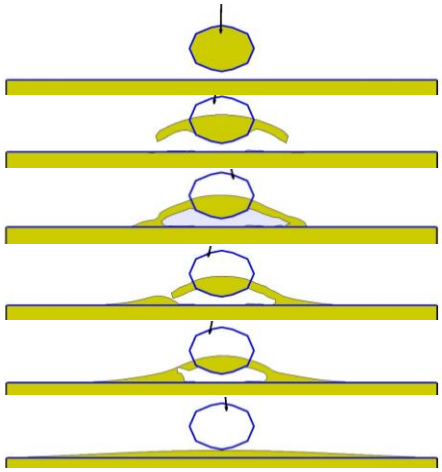

Figure 6 Subsequent stages in the island migration and merging test;

Flying spits

In order to test the model performance under a high angle of wave incidence, and to verify the model ability to grow spits through the instability mechanism according to (Ashton et al., 2001), the test conditions follow the numerical test introduced by (Kaergaard and Fredsoe, 2013a).

Initial condition	**Value**
Total shoreline length	100 km
Undulation with a length	5000 m
The amplitude of the undulation	50 m

Wave parameter	**Value**
Wave height	1 m
Peak wave period	5 sec
Mean wave direction	300°

For this test the initial grid size = 250 m, spit width=250 m, closure depth = 15 m and the CERC formula was applied; the total simulation time was 250 years.

Periodic boundary conditions were used to the right and Neumann boundary conditions on the left boundary; Figure 9 shows the 50 km in the middle at different stages. We

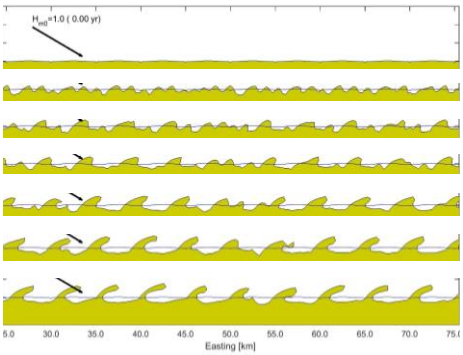

Figure 9 Shoreline undulations under test conditions of Kaergaard and Fredsoe, 2013.

clearly see the initial disturbances grow into wave-like patterns, which grow and merge into larger length scales, and finally reach the stage of flying spits, of which even small islands can be detached.

Van Rijn's bestiary of coastal forms

The following case is inspired by the picture in (van Rijn, 1998), see Figure 10. It describes a 'bestiary' of coastal features and our ambition was to re-create most of them in a single simulation.

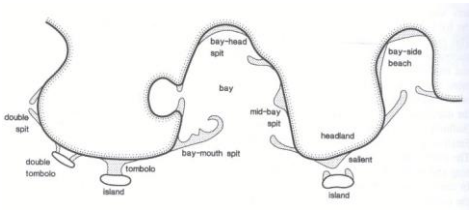

Figure 10 Overview of sandy coastal shapes, from van Rijn (1998)

The initial setup is shown in the top panel of Figure 11. It contains a coast with sharp variations in orientation with a sandy island and two hard offshore breakwaters or rocky obstacles. The wave climate is from the south with a random spreading of +/- 60°. We see a number of spits developing, on the sides of the island and on all protruding parts of the coast ('bay-mouth spits'). After 20 years the island spits weld to the coast creating a lagoon. The western breakwater captures the westward longshore transport, creating a tombolo. After 50 years the central spits merge together and start extending seaward, while the island has fully disappeared, its sand distributed along the eroding coast. On the western coast the headland spit has welded to the coast, creating a curved embayment with an enclosed lagoon.

These developments seem quite realistic and form an illustration of the capability of ShorelineS to represent not just incremental coastal changes, but radical transformations of the coast over long timescales.

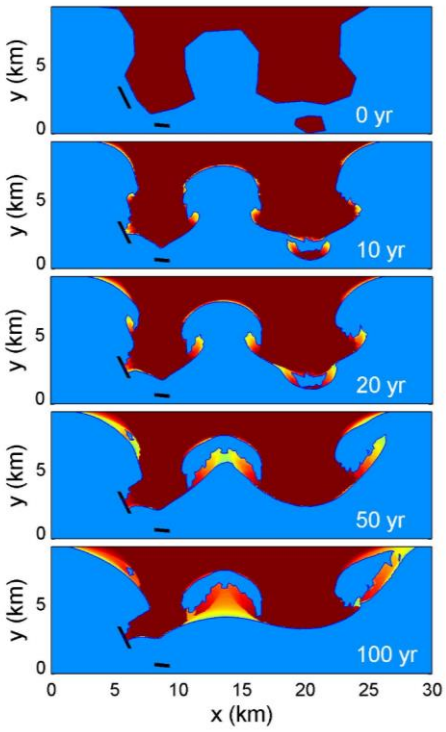

Figure 11 Evolution of coastal features in a geometry resembling van Rijn's overview of coastal shapes. Colours indicate age of deposition, with yellow the most recent deposition to dark red for the oldest deposition.

The colouring of **Error! Reference source not found.** is done through post-processing on a fine grid, where for each pixel we keep track of when it has become land or sea.

This representation facilitates a comparison with observed horizontal stratigraphic features such as beach ridges.

4. Analytical tests

A number of analytical tests were carried out to verify the correct implementation of the governing equations and the numerical scheme. They are described extensively in (Elghandour, 2018). Here, for brevity, we will summarize results for two of these tests.

Linear diffusion test

The first test is the verification test used by (Vitousek and Barnard, 2015) to validate his model. By comparing one analytical solution for the linear diffusion equation with the model. The shoreline starts with configuration $y = a\cos(kx)$ where $k = 4\pi / L$ and the analytical solution of the shoreline evolution is $y = a\exp\left(-\nu k^2 t\right)\cos\left(kx\right)$ where $\nu = 2Q_o / D_c$. The parameters for the test are explained and given values in Table 2.

Table 2 Parameters linear diffusion test

the amplitude of the shoreline perturbation(a)	100 m
domain length (L)	5 km
constant wave angle (α)	0
idealized form of transport rate (Q0)	10^5 m^3/yr
closure depth (D_c)	10 m
boundary condition (Q)	0 m^3/yr
Δ x	50 m
total simulation time	30 yr

The model was run with an adaptive time step based on the criterion $\Delta t < 2\nu / \Delta x^2$, and the resulting evolution is stable and accurate.

Pelnard-considère groyne test

This test reproduces the well-known analytical solution for the accretion and erosion on either side of a groyne on a uniform coast, according to (Pelnard-Considere, 1956). For the case where wave shadowing is turned off, the agreement is good even though the angle of 30° can hardly be called 'small'.

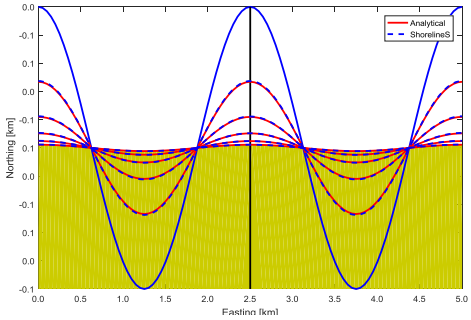

Figure 12 The diffusion test result using the adaptive time step; results shown every 6 years.

Results for the different formulas are extremely similar. The shadowing has the effect of shifting the pattern for this particular condition downdrift. The effect of diffraction is not yet included in this test, though it has been implemented and will be reported in a subsequent paper.

Overall we may conclude that the comparison with analytical testcases is satisfactory, both for the diffusion test and the groyne case, and that the basic equations and numerical scheme have been implemented correctly.

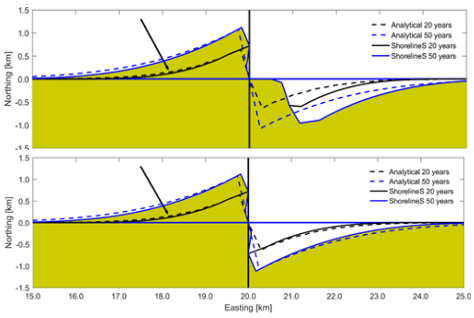

Figure 13 Coastline evolution on either side of a groyne, for wave incidence angle of 30 deg., with shadow effect (top) and without the shadowingl comparison with Pelnard-Considère (1956) solution after 20 resp. 50 years.

5. Field validation

Sand Engine

We illustrate the capability of ShorelineS to represent real-world developments through the example of the Sand Engine (Luijendijk et al., 2017; Stive et al., 2013). This has been the subject of intensive modelling efforts with 2DH

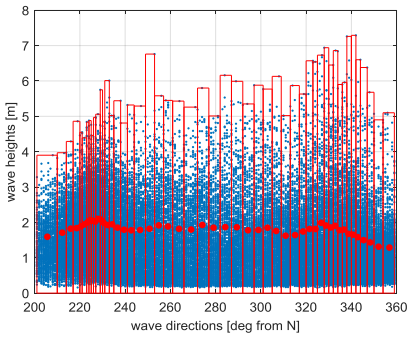

Figure 14 Wave climate based on observations in IJmuiden Munitiestortplaats

process-based models, 1D line models and hybrid approaches, all of which take up considerable time to set up, calibrate, run (run times of up to months) and require a high level of expertise. The results are reasonable after considerable tuning, but only the most expensive process-based approach leaves behind a lagoon after the spit has merged with the mainland. On the other hand, the ShorelineS model in its simplest form, as we have tested it for this case, requires only the initial, complex coastline and a nearby deep water wave climate. The latter is given as a probability distribution of (50) wave direction bins, each with equal total energy flux, with one wave height class per direction, as depicted in Figure 14, since we considered that an accurate representation of the directional wave climate is the most important aspect in the schematization. The initial model resolution was set at 100m. After tuning of the transport magnitude (formula CERC1, b=500,000 $m^{1/2}$/yr/rad, profile height 10m), which only influences the speed of developments (not the shape), the results shown in Figure 15 were obtained: a qualitatively correct and quantitatively good reproduction of the observed behaviour, at minimal runtime (approx. 15 min). Though this result is quite promising, the case will be studied much more in depth and reported more extensively in a subsequent paper.

6. Discussion

This paper presents the principles of a radically new coastline model concept and illustrates a number of capabilities. For simple cases its behaviour is comparable to existing coastline models; however, we show that it is able to represent much more complex situations. The principle tests show its strength in demonstrating coastal processes and in reconstructing geological planform records. A first validation with a complex real-world case (the Sand Engine) shows that the methodology has the potential to be used as an efficient engineering tool; cases such as the accretion on both sides of the harbour of IJmuiden, as described in (Roelvink and Reniers, 2011), are readily reproduced.

The model is extremely easy to run, as it merely requires initial coastline polylines, polylines of hard structures,

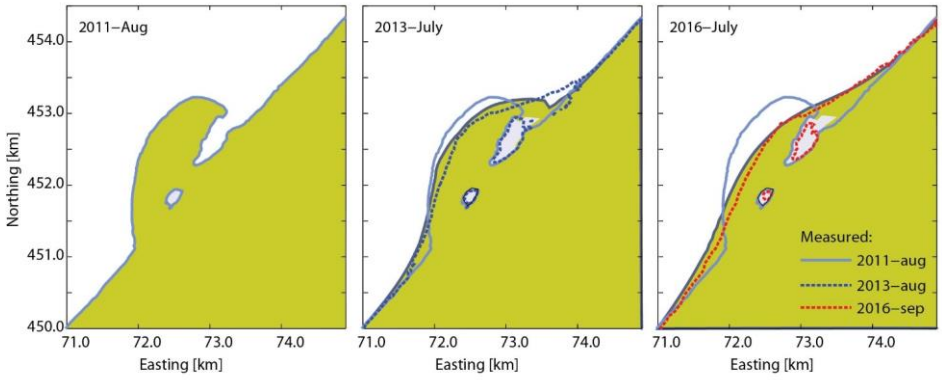

Figure 15 Observed and simulated evolution of the Sand Engine using ShorelineS; filled contours: snapshots of simulation result at start, after 2 years (middle) and 4 years (right). Colour-coded lines are coastlines extracted from repeat topo-bathy surveys.

offshore wave data and some parameter settings; data that is generally readily available through satellite imagery and global or regional wave hindcasts, or local wave data.

However, a large number of items remain on the to-do list, as will be outlined in the following sections.

7. Work in progress

Development is continuing on a number of issues as outlined below and regular updates will be posted on the open-source web link www.shorelines.nl.

Automatic timestep

In order to guarantee the robustness, given the explicit numerical scheme, an automatic time step has been implemented, which takes into account the characteristics of the different transport formulations implemented.

Inclusion of diffraction

Including the effect of diffraction and refraction behind offshore breakwaters and other hard structures or headlands is reported in (Elghandour et al., 2018b). This allows for an accurate description of the evolution of salient through to full tombolo's, made possible because of the free-form character of ShorelineS.

Large-scale wave refraction

For cases where important non-uniform wave refraction takes place between the deep water and the depth of closure, e.g. behind an underwater delta front, ebb delta or generally non-uniform offshore bathymetry we have implemented a fast implicit refraction model which propagates the offshore waves over a relatively coarse 2D grid and creates a lookup table; local wave conditions for ShorelineS are interpolated from this table. When relevant, the shoreline evolution can be made to feed back into the large-scale bathymetry; see (Elghandour et al., 2018a).

2-Way coupling with 2DH tidal morphodynamics

In the vicinity of tidal inlets, the tidal currents will obviously influence the behaviour of the coastlines on either side; here we may apply a two-way coupling between ShorelineS and a 2DH morphodynamic model such as Delft3D; the latter could be relatively coarse as it does not have to resolve the surf zone currents. Changes in coastline position feed back into the 2DH model by assuming a cross-shore profile shape; nearshore bathymetry changes computed by the 2DH model are 'felt' as sources or sinks in ShorelineS. This has been implemented, but much testing remains to be done, on aspects such as the frequency of interaction and details of the bathymetry updating.

8. Outlook

Barrier migration over pre-existing bathymetry/topography.

The active profile depth, usually taken as a constant, is determined in part by the wave climate, but also by the pre-existing bathymetry, for instance in the case of a spit expanding over a shallow bathymetry. We will develop estimates of antecedent bathymetry from global and local resources. Especially as we will be considering coastal evolution over many decades, landward propagation of coastal barriers over low-lying marshes or lagoons will be an important process to consider.

Cross-shore effects on event to decadal scales.

Although the primary forcing of the ShorelineS model is due to longshore transports, which in the long run dominate the shape of coastlines and their erosional or accretional trends, important contributions due to cross-shore transport act on three timescales. We envisage adopting increasingly sophisticated approaches to account for sea-level rise (Bruun effect, barrier rollover, basin infilling); seasonal changes due to wave energy variations(Yates et al., 2009) to keeping track of a set of cross-shore profile positions through Larson's Cross-Shore Model (CSM) approach(Larson et al., 2016).

Automatic model generation from satellite imagery

As was shown by (Luijendijk et al., 2018) it is now possible to generate, at longshore distances of approx. 200 m, time-series of coastline locations normal to the local coast direction; depending on the number of cloudy days, reliable observations with intervals of 2 to 6 months, with sub-pixel accuracy can be generated. This opens the way to automatically generate, anywhere, a base coastline for hindcast purposes, and shapes indicating the presence of rocky features and hard structures, as well as a time series of coastal evolution for calibration or assimilation of the model.

Probabilistic forecasting

Particularly for complex coastlines susceptible to radical changes during unpredictable extreme events, it is essential not to limit ourselves to a single deterministic run for a given scenario, but to carry out ensemble forecasts, where a number of realizations of the same scenario aregenerated, with variations in initial conditions, model parameters and/or boundary conditions time series. In addition, a coupling can be envisaged with the Probabilistic Coastline Recession model (PCR) (Ranasinghe, 2012) where we include the previously ignored long-term coastline trend based on the ShorelineS results.

References

Ashton, A., Murray, A.B., Arnoult, O., 2001. Formation of coastline features by large-scale instabilities induced by high-angle waves. Nature 414, 296-300.

Barbier, E.B., Hacker, S.D., Kennedy, C., Koch, E.W., Stier, A.C., Silliman, B.R., 2011. The value of estuarine and coastal ecosystem services. Ecological Monographs 81, 169-193.

Elghandour, A., 2018. Efficient modelling of coastal evolution. Development, verification and validation of ShorelineS model, Water Science and Engineering. IHE Delft Insitute for Water Education, Delft.

Elghandour, A., Huisman, B.J.A., Reyns, J., Roelvink, D., 2018a. Improving the wave description in the free-form coastline model ShorelineS: Part I, Large-scale refraction and effect on spit evolution. Coastal Engineering (in prep, preview available at www.shorelines.nl).

Elghandour, A., Huisman, B.J.A., Reyns, J., Roelvink, D., 2018b. Improving the wave description in the free-form coastline model ShorelineS: Part II Diffraction and effects on coastal evolution behind structures. Coastal Engineering (in prep, preview available at www.shorelines.nl).

Falques, A., Calvete, D., 2004. Large scale dynamics of sandy coastlines. Diffusitivy and Instability. J. Geophys. Res. 101, C03007.

Falqués, A., Ribas, F., Idier, D., Arriaga, J., 2017. Formation mechanisms for self-organized kilometer-scale shoreline sand waves. Journal of Geophysical Research: Earth Surface 122, 1121-1138.

Hanson, H.a.K., N.C., 1989. GENESIS: Generalized model for simulating shoreline change, Report 1. Technical Reference. DEPARTMENT OF THE ARMY Waterways Experiment Station, Corps of Engineers Technical Report CERC-89-19.

Hurst, M.D., Barkwith, A., Ellis, M.A., Thomas, C.W., Murray, A.B., 2015. Exploring the sensitivities of crenulate bay shorelines to wave climates using a new vector-based one-line model. Journal of Geophysical Research: Earth Surface 120, 2586-2608.

Idier, D., Falqués, A., Ruessink, B.G., Garnier, R., 2011. Shoreline instability under low‐angle wave incidence. Journal of Geophysical Research: Earth Surface 116.

Kaergaard, K., Fredsoe, J., 2013a. Numerical modeling of shoreline undulations part 1: Constant wave climate. Coast Eng 75, 64-76.

Kaergaard, K., Fredsoe, J., 2013b. A numerical shoreline model for shorelines with large curvature. Coast Eng 74, 19-32.

Kristensen, S.E., Drønen, N., Deigaard, R., Fredsoe, J., 2016. Impact of groyne fields on the littoral drift: A hybrid morphological modelling study. Coast Eng 111, 13-22.

Larson, M., Palalane, J., Fredriksson, C., Hanson, H., 2016. Simulating cross-shore material exchange at decadal scale. Theory and model component validation. Coast Eng 116, 57-66.

Lorenzo-Trueba, J., Ashton, A.D., 2014. Rollover, drowning, and discontinuous retreat: Distinct modes of barrier response to sea-level rise arising from a simple morphodynamic model. Journal of Geophysical Research: Earth Surface 119, 779-801.

Luijendijk, A., Hagenaars, G., Ranasinghe, R., Baart, F., Donchyts, G., Aarninkhof, S., 2018. The State of the World's Beaches. Scientific Reports 8, 6641.

Luijendijk, A.P., Ranasinghe, R., de Schipper, M.A., Huisman, B.A., Swinkels, C.M., Walstra, D.J.R., Stive, M.J.F., 2017. The initial morphological response of the Sand Engine: A process-based modelling study. Coast Eng 119, 1-14.

Pelnard-Considere, R., 1956. Essai de theorie de l'Evolution des Formes de Rivages en Plage de Sable et de Galets, 4emes Journées de l'Hydraulique, les Énergies de la Mer, Question III, Rapport No. 1, pp. 289-298.

Ranasinghe, R., Callaghan, D. P. and F., S. M. J. , 2012. Estimating coastal recession due to sea level rise: Beyond the Bruun rule. Climatic Change 110, 561-574.

Ranasinghe, R., Duong, T.M., Uhlenbrook, S., Roelvink, D., Stive, M., 2013. Climate-change impact assessment for inlet-interrupted coastlines. Nature Clim. Change 3, 83-87.

Roelvink, D., Reniers, A., 2011. A Guide to Modeling Coastal Morphology. World Scientific, Singapore.

Stive, M.J.F., de Schipper, M.A., Luijendijk, A.P., Aarninkhof, S.G.J., van Gelder-Maas, C., van Thiel de Vries, J.S.M., de Vries, S., Henriquez, M., Marx, S., Ranasinghe, R., 2013. A New Alternative to Saving Our Beaches from Sea-Level Rise: The Sand Engine. J Coastal Res, 1001-1008.

Syvitski, J.P., Vörösmarty, C.J., Kettner, A.J., Green, P., 2005. Impact of humans on the flux of terrestrial sediment to the global coastal ocean. Science 308, 376-380.

Tonnon, P.K., Huisman, B.J.A., Stam, G.W., Van Rijn, L.C., 2017. Numerical modelling of mega nourishments using coastline and coastal area models; design graphs for erosion rates, life span and maintenance volumes. Coast Eng (in review).

van Rijn, L.C., 1998. Principles of coastal morphology. Aqua Publications.

Vitousek, S., Barnard, P.L., 2015. A nonlinear, implicit one-line model to predict long-term shoreline change, Coastal Sediments 2015. ASCE, San Diego.

Yates, M.L., Guza, R.T., O'Reilly, W.C., 2009. Equilibrium shoreline response: Observations and modeling. Journal of Geophysical Research: Oceans 114, n/a-n/a.